

Key Factors Contributing to Two Pyrocumulonimbus Clouds Erupting During a Prescribed Burn in Western Australia.

Valerie S. Densmore *

Dept of Biodiversity, Conservation & Attractions, Manjimup, Western Australia, Australia,
valerie.densmore@dbca.wa.gov.au

Introduction

On 8th Nov 2017, two pyrocumulonimbus clouds (pyroCb) formed over a prescribed burn conducted near Rocky Gully in southwest Western Australia. The Table Hill burn (FRK_053) was conducted over the 6th – 9th Nov and targeted two adjacent cells of primarily jarrah (*Eucalyptus marginata*) and marri (*Corymbia calophylla*) open forest. The first pyroCb formed when the eastern cell was being edged on 8th Nov, producing thunder and lightning and prompting rapid fire spread that burned around two thirds of the 7953 ha cell in around 5 hours. A second pyroCb erupted approximately 6 hours after the first and significantly amplified fire behaviour, caused multiple hopovers over two boundaries and increased the risk to fireground personnel. The formation of two pyroCbs is uncharacteristic of prescribed burns, which are intended to mitigate rather than create extreme fire behaviour. This event prompted a review to identify the key factors that facilitated or triggered the pyroCbs to help define what parameters will prevent a reoccurrence of plume-driven fire activity at a prescribed burn.

Pyrocumulonimbus clouds are essentially cumulonimbus (i.e., thunderstorm) clouds that use heat from a fire to generate lift. In simple terms, pyroCbs require a conditionally unstable atmosphere and sufficient lift to release the instability. Several factors are strongly suspected to help trigger a pyroCb. These factors include: a significant volume of fire-heated air is lifted to the level of free convection (LFC); a source of moisture from the environment, fuel and/or combustion; a dry well-mixed lower layer overlaid by a moist middle troposphere; a near-surface wind surge from a thunderstorm, cold front, sea breeze, or boundary-layer roll; warm moist air remaining buoyant to the LFC, which generally entails a large, intense heat source and low surface wind strength. Notably, rotating plumes have less entrainment and increase the likelihood of reaching the LFC (Tory and Thurston 2015).

A recurring theme is that air must have sufficient lift to reach the tropopause. In general, a deep flaming zone (e.g., a large fire) is needed to produce and sustain the initial lift (McRae *et al.* 2015). The heat generated while edging a prescribed burn wouldn't be expected to produce enough lift unless other features like topography and/or plume dynamics supplemented fire behaviour or air buoyancy. To determine the primary factors that supported or permitted the pyroCbs to erupt, a review was conducted to analyse ignition patterns, the path and behaviour of the burn, weather conditions and models of surface fire behaviour (Spark) and pyroCb fire power threshold (FPT). This reconstruction helps highlight the contribution of fuel, terrain, weather and atmospheric factors to determining fire behaviour. The analysis also seeks to identify triggers that can support operational decisions when burning complex terrain and/or in unfavourable climates.

Location and Site Description

The Table Hill burn (FRK_053) was located approximately 11 km S of Rocky Gully and 41 km NE of Walpole in southwestern Western Australia. The burn contained a 3013 ha western cell and 7953 ha eastern cell, and this review concerns the larger eastern cell. The area has a Mediterranean-type climate with warm dry summers and cool wet winters. The long-term average annual rainfall is 715 mm occurring over an average of 105 days, predominately during May through September. Long-term average rainfall in November is 37.7 mm, and average temperature and relative humidity (RH) in November at 1500 hrs are 20.7 °C and 53%.

Terrain

The eastern cell contained several distinct hills dispersed along multiple valleys (Fig 1A). Notably, one valley crossed the N boundary at three locations and another valley connected the S to the lower W boundaries. Such terrain could channel wind, increasing speeds and changing directions from prevailing conditions. Most of the hills had slopes ranging from 6° - 14°, and any wind direction would face multiple slopes. Every 10° increase in slope will double a fire's rate of spread upslope, and the lee-side of slopes can experience turbulence in strong winds.

Vegetation and fuel characteristics

Vegetation type and structure corresponded to topographical features (Fig 1B). Vegetation was predominately open forests of mixed jarrah and marri at 10 – 30 m growing on mild to steep granite slopes with a moderately dense mid-storey at 1 – 6 m and moderately dense understorey of woody shrubs up to 1 m height. The burn also contained low woodlands and shrublands with heath species at 0.5 – 2 m, and relatively dense sedgeland, which were likely still moist when the burn was implemented.

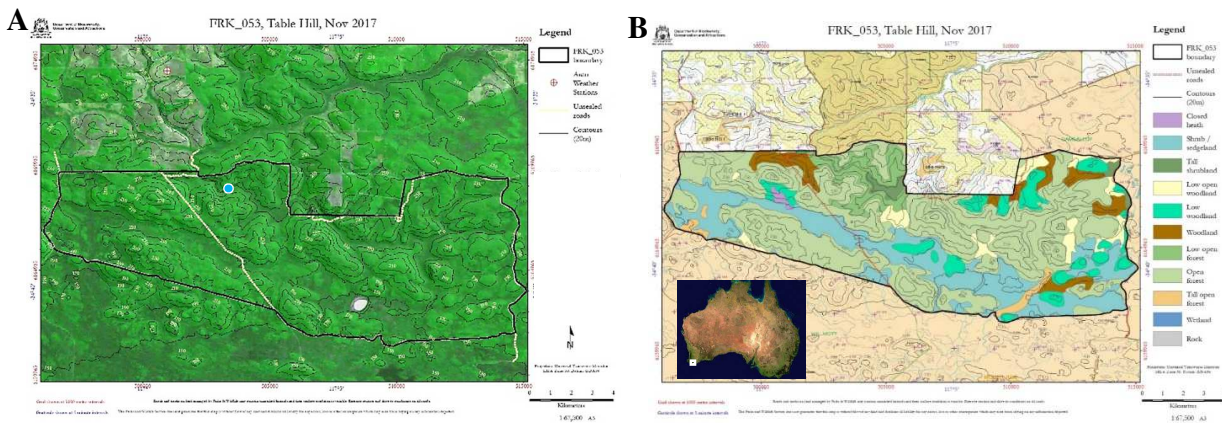


Figure 1. Terrain (A) and vegetation types (B) within the FRK_053 burn boundary with 10 m contour lines. The blue circle in (A) shows the location of a water gauging station. Inset in (B) shows the burn location (white box) within Australia.

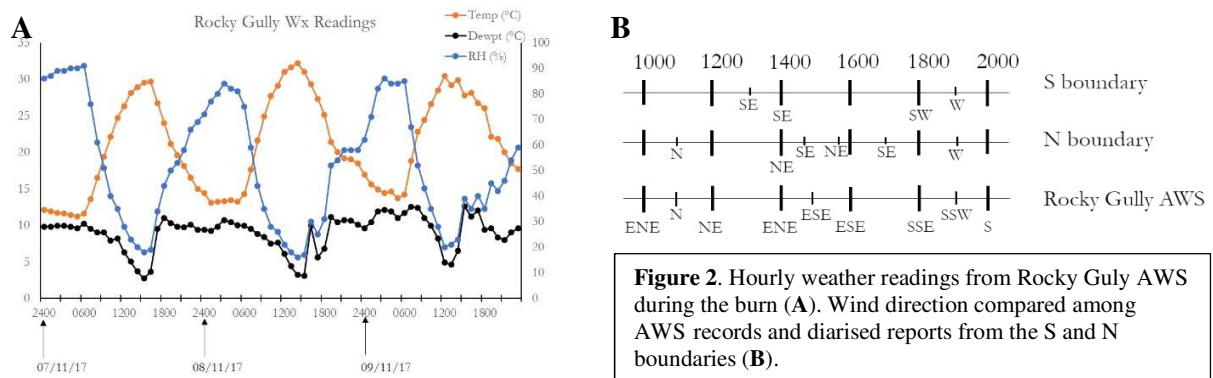
Most of the vegetation was 9 years old with scattered pockets of 13 – 14 year-old fuel. The predominant fuel age fit the regional fire management guidelines of a low intensity burn every 6 – 10 years in jarrah forest (WRFMS 2016). Available and total fuel loads were calculated between 13 – 17 tha^{-1} and 19 – 22 tha^{-1} , respectively, using forest fire behaviour tables for Western Australia (Sneeuwjagt and Peet 2008). Fine fuel moisture (SMC) was measured at 7% on the morning of 8th November using a Wiltronics moisture meter. Daily minimum SMC values below 10% can increase the rate of spread by a factor of 1.8 – 2.1 (Sneeuwjagt & Peet 1985).

Surface and synoptic weather

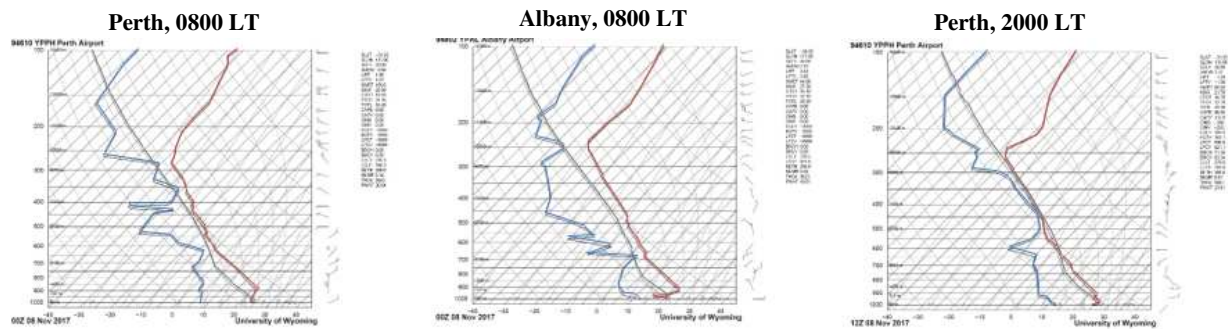
Australian Bureau of Meteorology (BOM) duty forecasters daily prepared localised weather forecasts that included temperature, RH, dewpoint, and wind speed (km h^{-1}) and direction at 10 m AGL in 3-hourly intervals from 0900 to 0300 hrs the next day. An automatic weather station (AWS) approximately 5 km N of the burn recorded prevailing conditions at hourly intervals (Fig 2A). The AWS readings were likely delayed by 30 – 60 minutes relative to the S boundary due to its location and comparisons made to diarised weather notations (Fig 2B).

Wind direction deviated from what was forecast. Winds on 8th Nov were predicted to remain between N'ly to E'ly, but the spot forecast included a warning that “variable direction wind gusts to 80 km/h (were) possible in and near thunderstorms.” A SE'ly wind reached the burn by 1330 local time (LT). Winds shifted from ESE to SSE to SSW between 1700 – 1900 LT. It is worth

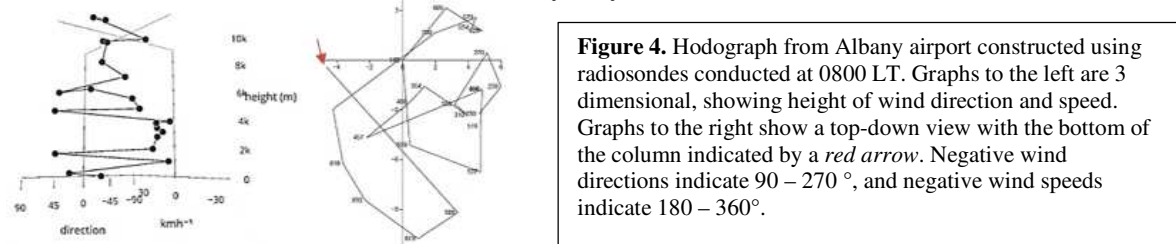
noting that diarised records of wind direction varied across the burn during the afternoon of 8th Nov (Fig 2B).



Aerological diagrams from both Perth and Albany showed an elevated risk of convective activity at 0800 LT on 8th Nov (Fig 3). Albany and Perth airports were ~ 65 km SE and 250 km NW of the burn, respectively. Thunderstorm activity was forecast, free convection was distinctly possible above 3500 m, and the atmosphere held more precipitable water, promoting a rapid rise to the LFC (Jenkins 2004). The inverted-V shape associated with previous pyroCbs can be seen on three radiosondes on 8th Nov (Tory and Thurston 2015). The c-Haines value was 9.3, indicating an unstable atmosphere (Mills and McCaw 2010).



Hodographs from 8th Nov showed wind directions changing up the atmospheric profile in a way that might create a natural vortex (Fig 4). Aerial photographs taken along the S boundary on the 8th show somewhat narrow columns that appear to have a twisting motion. This observation fits with light upper level winds changing direction, supporting free convection and the possible formation of a vortex (Potter 2012). The pyroCb erupted approximately 90–100 min after edging commenced on 8th Nov. This rapid development indicates the atmosphere played an active rather than passive role to create plume buoyancy.



Reconstruction and Analysis

A chronology of events including the timing and sequence of ignitions (Fig 5A), operational decisions and fire behaviours was compiled using fire diaries, interviews with fireground personnel and field surveys.

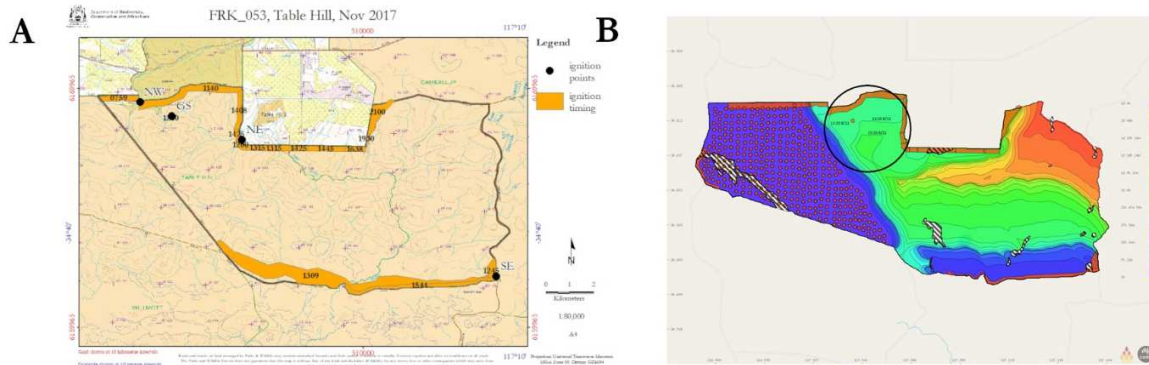


Figure 5. Actual ignition sequence and timings and fire spread as projected by the Spark surface model. (A) Ignition points for each sector are shown as a black dot. Orange bars represent ignition sequences, with the finish time overlaid. (B) Projected isochrones in 2-hourly increments and timeline from ignition to conclusion. Cross-hatched areas remained unburnt.

Although an unstable atmosphere was forecast, fuel ages surrounding the burn were 0 – 5 years, decreasing the risk the burn would escape. The S boundary was edged by hand on 7th Nov against a prevailing N wind. The ignition pattern was a series of 100 m lines introduced gradually to prevent ‘junction zones’ between ignition points that could elevate fire behaviour and throw firebrands across the boundary. This edging was active and deepened to over 200 m overnight.

On 8th Nov, the objective was to edge the N and then E boundaries to secure the burn. The N boundary was divided into an eastern and western sector spaced 3 km apart. A third site was located ~750 m south of the N boundary around a gauging station that otherwise aligned with the western sector (Fig 5A). Around 1030 LT, crews began placing spots 100 – 300 m apart along the eastern sector and around the gauging station. Around 1140, edging commenced using short continuous lines along the western sector north of the gauging station. Fire behaviour increased under a N’ly wind, and by 1200 LT, spots in the eastern sector were joining up and running back out to the boundary, so the decision was made to gradually implement a full line. Around 1215 LT, S’ly winds were detected approximately 42 km SW of the burn after two spots had been introduced on the E boundary, prompting lighting to be halted along the E boundary. Around 1315, lightning was seen in the smoke plume, accompanied by a loud thunderclap.

A series of infrared images from the Himawari 8 satellite suggest the size of the area alight more than doubled between 1130 and 1210 LT, when the first pyroCb erupted (Fig 6). This area corresponded to edging along the N boundary that resembled multiple strip ignitions in a hilly landscape. This lighting pattern could have enabled the convergence of heat and firelines. Each site was associated with a moderate slope (>10%). The slope on the western sector was on the lee side of prevailing NE’ly winds, supporting lee-side turbulence that could increase spotting and shift the dynamics of spread from a lineal to an areal pattern, characteristic of deep flaming (Peace *et al.* 2017). Deep flaming produces a significant amount of heat that gives buoyancy to the smoke plume (Sharples *et al.* 2012, McRae *et al.* 2015). Multiple strip ignitions are also more likely to support the formation of a vortex in the smoke plume (Potter 2012).

The infrared series shows a band between the gauging station and the western sector followed by a band connecting the eastern sector to the west. This becomes visible at 1200 LT as part of a large heat signature that would be a necessary precursor to the pyroCb that erupted 10 min later.

At 1210 LT, the heat signature extends abruptly southwest corresponding to a connecting valley. By 1300 LT, the two spots introduced on the E boundary appear to have joined up with edging along the S boundary. Infrared and leaf freeze patterns suggested wind channelling helped rapidly spread fire and increased fire intensity. Elevated fire activity was detected by infrared imaging from 1700—1750 LT. The orientation of this activity and leaf freeze patterns suggests it corresponded to a shift in prevailing winds from SSE to SSW. This wind change allowed a flank fire to become a head fire and aligns temporally to the second pyroCb erupting around 1653 LT.

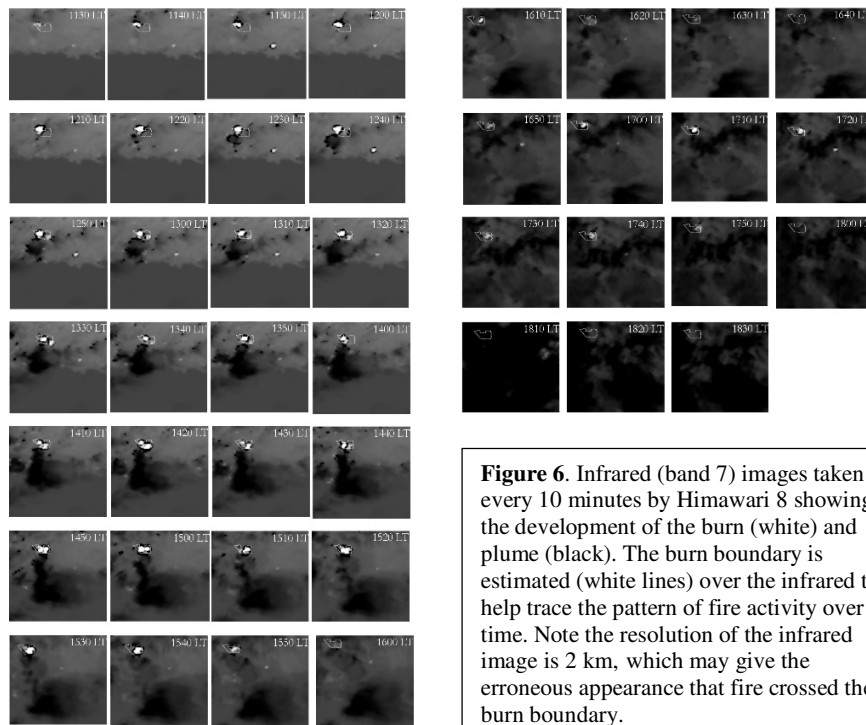


Figure 6. Infrared (band 7) images taken every 10 minutes by Himawari 8 showing the development of the burn (white) and plume (black). The burn boundary is estimated (white lines) over the infrared to help trace the pattern of fire activity over time. Note the resolution of the infrared image is 2 km, which may give the erroneous appearance that fire crossed the burn boundary.

Spark

Surface fire behaviour / path were modelled by James Hilton using the Spark model (Swedosh *et al.* 2018). The Spark output overpredicted by 24 hours the time needed to burn the cell from the edging that was introduced. The pattern of fire spread (Fig 5B) suggests a convergence of fire (*black circle*) in the NW corner from edging conducted around the gauging station and the two sectors on the N boundary. The fire was projected to have then spread southwards near the W boundary of cell 2 to join with fire spreading from the two spots introduced on the E boundary, in agreement with the infrared imagery shown in Figure 6.

PFT analysis

An analysis of pyroCb firepower threshold (PFT) was done by Kevin Tory at 6-hourly intervals to assess atmospheric support for pyroCb formation (Tory 2018). When PFT values fall below 100 gigawatts (GW), it suggests conditions are favourable for pyroCbs to form if sufficient heat is generated by a fire. The analysis suggested that PFT values were between 50 - 100 by 0800 hrs on the 8th. By 1400 hrs, the diagnosed PFT values were below 50 GW, suggesting very favourable conditions that required a much lower trigger, such as coalescence of fire lines or fire runs upslope, in order for a pyroCb to develop.

Discussion

A pyroCb occurring at a prescribed burn is highly unusual as burns are deliberately lit at a preselected date and time. The primary factors underlying the pyroCb eruptions were likely

terrain, fuel dryness and atmospheric instability. Although the terrain was steep enough to have multiplied fire behaviour, it was impossible to eliminate as a risk without cancelling the burn altogether, so other methods of controlling the risk needed to be implemented. Appropriate mitigation measures might have included highlighting the potential for accumulative risk in the burn prescription. This would facilitate the second step of adjusting the prescribed limits of factors that affect rate of spread, such as fire danger index and fine fuel moisture.

The Table Hill burn illustrated that a stable atmosphere is also critically important when burning in complex terrain. The western cell contained a river valley, hilly terrain and low fuel moisture (~8% SMC) but did not produce a blow-up fire when it was burned on 6—7th Nov. However, the atmosphere was stable during core ignition, thus the lift generated by heat and terrain did not reach the level of free convection. In contrast, most of the eastern cell was lit when the atmosphere was unstable. Timing of the first pyroCb also corresponded to the passage of a cloud band over the burn.

By determining the key factors that contributed to the pyroCbs, this analysis provides an opportunity to identify pivotal decisions and triggers to remember for future burns. The pivotal decisions centred around deciding to implement the burn when fuels were dry and unstable conditions were forecast. It is clear that the cumulative effects of terrain, SMC and atmospheric instability were not fully understood. Sources of elevated risk were steep slopes, multiple hills, linking river valleys, SMC<10%, unstable atmosphere forecast and approaching frontal systems. It is recommended these factors be specifically identified in burn prescriptions for additional comprehension, particularly when quick decisions need to be made during busy periods.

Acknowledgements

From DBCA: Neil Burrows, Lachie McCaw, Ali Raper, Tristan Farmer, Kerri-Ann Hudson, George Doust, Janine Liddelow, Wes Bailye, Paul Rampant, and Stefan Cannon. Mike Fromm (US Naval Research Labs), René Servranckx (Canadian Meteorological Centre), Rick McRae at (ACT Emergency Services Agency), Bradley Santos, Ivor Blockley, Mika Peace and Kevin Tory (BOM), Jason Sharples (UNSW), and James Hilton (CSIRO) for input, imagery and data

References

Gould JS, McCaw WL, Cheney NP, Ellis PF, Matthews S (2007) Field Guide - Fuel assessment and fire behaviour prediction in dry eucalypt forest. Ensis-CSIRO, Canberra, ACT and Dept Env Cons, Perth, WA.

Jenkins MA (2004) Investigating the Haines Index using parcel model theory. *Int J Wild Fire*. 13:297–309.

McRae RHD, Sharples JJ, Fromm M (2015) Linking local wildfire dynamics to pyroCb development. *Nat Haz Earth Sys Sci*. 15:417–428.

Mills GA, McCaw L (2010) Atmospheric stability environments and fire weather in Australia – extending the Haines Index. CAWCR, Technical report 20. The Centre of Australian Weather and Climate Research: Melbourne, Vic., Australia.

Sharples J, McRae R, Wilkes S (2012) Wind-terrain effects on the propagation of large wildfires in rugged terrain: fire channelling. *Int J Wild Fire*. 21:599—614.

Sneeuwjagt RJ & Peet GB (1985) Forest fire behaviour tables for Western Australia. Dept Cons Land Manag, Perth, WA.

Tory KJ & Thurston W (2015) Pyrocumulonimbus: a literature review. Bushfire Nat Haz CRC Report No. 2015067

Tory K (2018) Models of buoyant plume rise. Melbourne: Bushfire Nat Haz CRC

Warren Region Fire Management Service (WRFMS) (2016) Warren Regional Fire Management Plan 2016 – 2020. Dept Parks & Wildlife, WA.